

Fatigue crack growth characteristics of a new Ni–Co-base superalloy TMW-4M3: effects of temperature and load ratio

Zhihong Zhong · Yuefeng Gu · Toshio Osada ·
Yong Yuan · Chuanyong Cui · Tadaharu Yokokawa ·
Toshimitsu Tetsui · Hiroshi Harada

Received: 19 April 2011 / Accepted: 20 June 2011 / Published online: 29 June 2011
© Springer Science+Business Media, LLC 2011

Abstract The fatigue crack growth (FCG) behavior of a newly developed Ni–Co-base superalloy TMW-4M3 has been investigated in this study. Experiment was carried out in laboratory air with compact-tension specimen. The effects of temperature (400, 650, and 725 °C) and load ratio (0.05 and 0.5) on crack growth rate were studied in the Paris regime. The results revealed that the crack growth rate increased with increasing temperature under a given load ratio. The influence of load ratio on crack growth rate was pronounced, especially at higher temperature and low stress intensity factor range. Fractographic observations showed that fracture mode was transgranular at 400 °C, mixed transgranular and intergranular at 650 °C, and predominantly intergranular at 725 °C. The possible explanations for the crack growth behavior were discussed based on the degradation of mechanical properties and the oxidation assisted crack growth, as well as the crack closure effect. A comparison of FCG rate was also made between TMW-4M3 and the commercial superalloy U720Li.

Introduction

Ni-base superalloys have been widely used as turbine materials for both aerospace and land-based power

generation applications. The development of such alloys has been driven by the increasing demands for more efficient engine operation with higher operating temperatures and stresses. This has led to considerable efforts that have been undertaken on the design and development of new alloys and new processes [1]. Recently, the newly developed Ni–Co-base superalloys, namely TMW alloys, which are designed based on the commercial alloy U720Li by the National Institute for Materials Science, Japan, have emerged as attractive materials for turbine disk applications [2]. These alloys were developed to improve the hot working windows and enhance the volume fraction of strengthening precipitates. Among these TMW alloys, TMW-4M3 is a typical one that exhibits superior performances in microstructural stability [3] and tensile and creep properties [4, 5] as compared to U720Li. However, a critical property for such applications of TMW-4M3, fatigue crack propagation resistance, particularly at anticipated service temperatures (400–700 °C), has not been investigated yet.

Usually, the structural metals and alloys may contain small defects such as cracks, flaws (pores and inclusions), and machined marks which may impair their performance by causing the initiation and propagation of cracks during operation. It has long been recognized from the failure analysis that fatigue is one of the major causes of failure in cyclically loaded engineering structures like aircraft engine. Therefore, the investigation on fatigue crack growth (FCG) behavior and establishment of life-prediction methodologies for turbine disks are essential. This also gives rise to useful information for alloy design and process improvement. Good resistance to fatigue crack propagation is important for engine materials, since a crack once present must not propagate to failure between inspection intervals during a component's service. Therefore, there is an impetus to characterize the TMW-4M3 in

Z. Zhong (✉) · Y. Gu · T. Osada · Y. Yuan · T. Yokokawa ·
T. Tetsui · H. Harada
High Temperature Materials Unit, National Institute
for Materials Science (NIMS), 1-2-1 Sengen, Tsukuba,
Ibaraki 305-0047, Japan
e-mail: zhong.zhihong@nims.go.jp

C. Cui
Institute of Metal Research, China Academy of Science,
Shenyang 110016, China

terms of its resistance to crack propagation (especially in the Paris regime) and to make a contribution to its database for industrial applications.

Since both temperature and load ratio [6–8] are known to greatly influence FCG rate in metallic materials and alloys, efforts have been made in this study to evaluate the crack propagation behavior of TMW-4M3 at different temperatures up to the upper bound operating temperature, 725 °C, using variable load ratios, in the Paris regime.

Materials and experimental procedure

Material and tensile test

The nominal chemical compositions of TMW-4M3 alloy are given in Table 1. For comparison, the compositions of U720Li are also tabulated in Table 1. As can be seen from this table, the chemical compositions of TMW-4M3 are similar to that of U720Li but with a higher Co content and Ti/Al ratio and a lower Cr content. The higher Co content and higher Ti/Al ratio in TMW-4M3 is expected to favor the improvement of tensile strength and creep resistance. A reduced amount of Cr is expected to prevent the formation of σ phase after long-time thermal exposure of temperature higher than 700 °C [9]. The specimens used in this study were fabricated by a conventional cast and wrought route including triple melting, billet making, and pancake forging at Mitsubishi Materials Corporation, Japan. The solution heat treatment was conducted to achieve a fine grain before a duplex aging heat treatment for the alloy. The pancake-shaped alloy (440 mm in diameter and 65 mm in thickness) was subjected to the heat treatment (1100 °C/4 h/oil quenching, then aging at 650 °C/24 h/air cooling + 760 °C/16 h/air cooling). The specimens for tensile and FCG tests were machined from the heat-treated pancake. Optical microscopy (OM) and transmission electron microscopy (TEM) were used to examine the microstructural characteristics.

Before the FCG testing, the elevated temperature tensile properties of TMW-4M3 including the yield strength (σ_y), ultimate tensile strength (σ_u), percent elongation (%El), percent reduction in area (%RA), and Young's modulus (E) were determined at temperatures of 400, 650, and 725 °C using smooth cylindrical specimens according to the ASTM standard E21 [10].

Table 1 Nominal chemical compositions (weight percent) of TMW-4M3 and U720Li

Alloy	Ni	Co	Cr	Mo	W	Al	Ti	C	B	Zr
TMW-4M3	Bal.	25.0	13.5	2.8	1.2	2.3	6.2	0.02	0.02	0.03
U720Li	Bal.	15.0	16.0	3.0	1.3	2.5	5.0	0.02	0.02	0.03

FCG test

Compact-tension specimens (width of 50.8 mm and thickness of 12.7 mm) were machined from the heat-treated pancake (away from the center of the forging) for FCG rate tests. The crack plane was perpendicular to the circumferential direction and crack growth in the radial direction. FCG tests were conducted at Kobe Materials Testing Laboratory [4]. Before the elevated temperature FCG testing, specimens were precracked by fatigue at room temperature with a frequency of 20 Hz to a precrack length of 2.5–3 mm (crack length about 18 mm). FCG tests were carried out on a computer-controlled, closed-loop servo-hydraulic testing machine, in accordance with ASTM standard E-647 [11], with specimens cycled under load controlled condition. Tests were conducted in laboratory air at temperatures of 400, 650, and 725 °C, with a frequency of 2 Hz (a symmetric, triangular waveform). The effect of load ratio R (ratio of minimum to maximum loads) was also evaluated at values of 0.05 and 0.5.

The crack length was recorded by a capacitance gauge mounted across the notch mouth. The stress intensity factor (K) is determined according to ASTM E-399 [12] with a linear-elastic solution, as given by Eq. 1

$$K = \frac{F}{B\sqrt{W}} \left(\frac{2 + \alpha}{(1 - \alpha)^{3/2}} \right) \times [0.886 + 4.64\alpha - 13.32\alpha^2 + 14.72\alpha^3 - 5.6\alpha^4], \quad (1)$$

where F is the applied load, B is the specimen thickness, $\alpha = a/W$, where a is the crack length and W is the specimen width. FCG tests were started at a stress intensity factor range (ΔK) level of about 11 MPa $\sqrt{\text{m}}$ and were continued with α of about 0.35–0.7 (or about 18–35 mm of crack length) within the range specified in the standard [11]. Thus, although the fatigue tests ended before the specimen was pulled apart, a few data at the end of test ($\alpha > 0.7$) were removed, because these data points correspond to the crack growth with a mixture of tensile and shear modes. Results are presented in terms of the crack growth rate per cycle (da/dN) as a function of ΔK . The fracture surface of the specimen was examined by scanning electron microscopy (SEM) operated at 20 kV.

Results

Microstructural characterization and tensile properties

The microstructures of TMW-4M3 alloy is shown in Fig. 1. The subsolvus solution temperature of 1100 °C produced a microstructure with a fine mean grain size

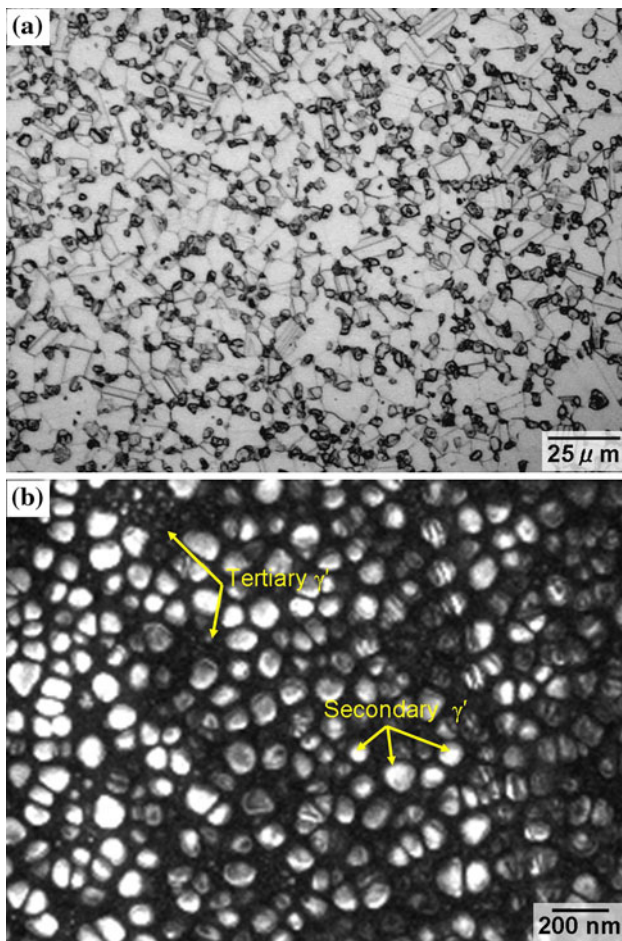


Fig. 1 **a** Optical micrograph and **b** transmission electron micrograph (dark field image) showing the grain structure and distribution of γ' precipitates of TMW-4M3

(8.7 μm) and generated an uniform distribution of un-dissolved primary gamma prime (γ') precipitates with a size of 0.5–2.3 μm , between the gamma (γ) grains or in the interior of grains (Fig. 1a). The volume fraction of primary γ' was about 16.9%. Aging twins were also discernible within some grains. In addition, small quantities of M_{23}C_6 or MC carbides ($\sim 0.5\%$) were also present at grain boundaries. Very fine secondary (30–100 nm in diameter) and tertiary γ' (5–10 nm) particles precipitated in γ grain can be seen in Fig. 1b.

The tensile properties of TMW-4M3 as a function of the testing temperature are given in Table 2. The σ_u decreased drastically above 650 $^\circ\text{C}$, but σ_y decreased slightly from

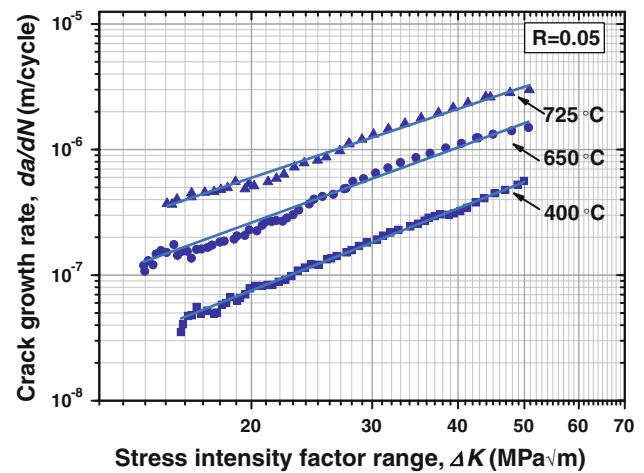


Fig. 2 FCG rate, da/dN , as a function of ΔK , for TMW-4M3 tested under different temperatures with a load ratio of 0.05

400 to 725 $^\circ\text{C}$. Young’s modulus (E) and ductility in terms of %EI and %RA showed similar trend as that observed in σ_y , i.e., the magnitude of these properties were gradually reduced with increasing temperature. The decrease in E indicates that the stiffness reduced at higher temperatures and the changes in mechanical properties could have an influence on the FCG behavior.

FCG behavior

Effect of temperature on FCG rates

The influence of temperature on the FCG as a function of ΔK at 400, 650, and 725 $^\circ\text{C}$ under a load ratio of 0.05 is shown in Fig. 2. It needs to be noted that the near-threshold and the very high growth rate regimes corresponding to crystallographic cracking and a static rupture mode, respectively, have not been investigated in this study. It is clear that increasing the test temperature from 400 to 725 $^\circ\text{C}$ resulted in significant increase in crack growth rates at all levels of ΔK . For example, at a ΔK level of 20 $\text{MPa}\sqrt{\text{m}}$, the FCG rate at 725 $^\circ\text{C}$ was a factor of 7 higher than that at 400 $^\circ\text{C}$ and about four times higher than that at 650 $^\circ\text{C}$. In addition, the differences in FCG rates under the same ΔK tested between 400 and 650 $^\circ\text{C}$ were kept almost constant at all levels of ΔK up to 50 $\text{MPa}\sqrt{\text{m}}$. However, such differences tested between 650 and 725 $^\circ\text{C}$ were decreased with increasing the ΔK . At ΔK level of 20

Table 2 Tensile properties of TMW-4M3

Temperature ($^\circ\text{C}$)	σ_y (MPa)	σ_u (MPa)	%EI	%RA	E (GPa)
400	1102 \pm 14	1560 \pm 4.0	14.8 \pm 1.4	15.3 \pm 1.5	207 \pm 2.1
650	1074 \pm 7.3	1400 \pm 7.1	13.6 \pm 2.5	12.9 \pm 0.6	190 \pm 2.6
725	1047 \pm 19	1177 \pm 9.9	10.6 \pm 0.6	12.5 \pm 0.1	183 \pm 3.0

and $50 \text{ MPa}\sqrt{\text{m}}$, for instance, the FCG rate at $725 \text{ }^\circ\text{C}$ was about four times and two times higher than that at $650 \text{ }^\circ\text{C}$, respectively.

The sensitivity of the crack propagation rate to changes in stress intensity could be reflected by a material constant, m , contained in the well-known Paris law as follows:

$$da/dN = C(\Delta K)^m, \quad (2)$$

where, a is the crack length, N is the number of cycles, da/dN is the crack growth rate, and C is a constant. C and m are constant depending on material and environment, and were determined by linear regression of $\log(da/dN)$ and $\log(\Delta K)$ data for each test temperature. The results are summarized in Table 3. Two different crack growth behaviors were noted from this table. First, at the lower temperature range, from 400 to $650 \text{ }^\circ\text{C}$, with almost the same m value; and second, at the higher temperature range, about $650 \text{ }^\circ\text{C}$ and higher, where m decreased with increasing temperature. This may indicate a change in fracture mechanism. The effect of temperature on FCG rate may also be seen in the Arrhenius plot of Fig. 3. Two distinct slopes, one at lower temperatures and the other at higher temperatures, could be seen and that is suggestive of two different mechanisms.

Table 3 Material constants C and m determined from da/dN versus ΔK plots for TMW-4M3

Temperature ($^\circ\text{C}$)	$R = 0.05$		$R = 0.5$	
	C	m	C	m
400	9.12×10^{-11}	2.23	1.98×10^{-10}	2.04
650	3.76×10^{-10}	2.16	1.15×10^{-9}	2.03
725	1.95×10^{-9}	1.89	4.19×10^{-8}	1.18

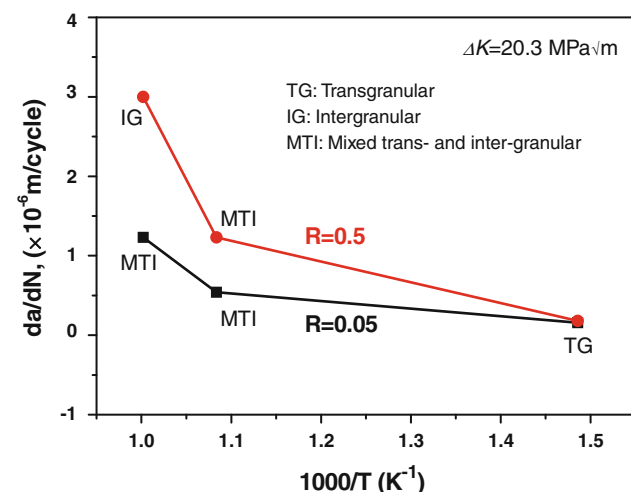


Fig. 3 Arrhenius plots of crack growth rates taken at $\Delta K = 20.3 \text{ MPa}\sqrt{\text{m}}$

Effect of load ratio on FCG rates

The influence of load ratio (R) on FCG rates is presented in Fig. 4. At each test temperature, the crack growth rate increased when the load ratio increases from 0.05 to 0.5 . Furthermore, the effect of load ratio is more pronounced at higher temperatures (650 and $725 \text{ }^\circ\text{C}$) as compared to that at $400 \text{ }^\circ\text{C}$, especially at lower ΔK levels ($<30 \text{ MPa}\sqrt{\text{m}}$). m values were also calculated for $R = 0.5$ test (Table 3). It is noted that for the tests carried out at $725 \text{ }^\circ\text{C}$, m ($m = 1.18$) roughly half the value observed at $400 \text{ }^\circ\text{C}$ ($m = 2.04$). A significant difference in the slope between $725 \text{ }^\circ\text{C}/R = 0.5$ and other tests are indicative of a change in FCG mechanisms at the crack tip. A decrease in the slope indicates that a material is relatively insensitive to the change in ΔK . The possible explanations for this phenomenon will be discussed on the basis of fractographic observation.

Fractography

Test under load ratio of 0.05

The effects of temperature and load ratio on FCG rate were accompanied by a change in fracture mode which could be examined from the fracture surfaces. Fracture surfaces corresponding to $\Delta K = 20$ and $40 \text{ MPa}\sqrt{\text{m}}$ regime of TMW-4M3 when tested at $400 \text{ }^\circ\text{C}$ are presented in Fig. 5b, c, respectively. The mode of fracture under cyclic loading in both regimes appeared to be a transgranular mode. Very fine fatigue striations were observed on the fracture surfaces, indicating a pure FCG mechanism that is controlled by duplex slip processes [13]. At $\Delta K = 40 \text{ MPa}\sqrt{\text{m}}$ regime, a more textured fracture morphology with cracks

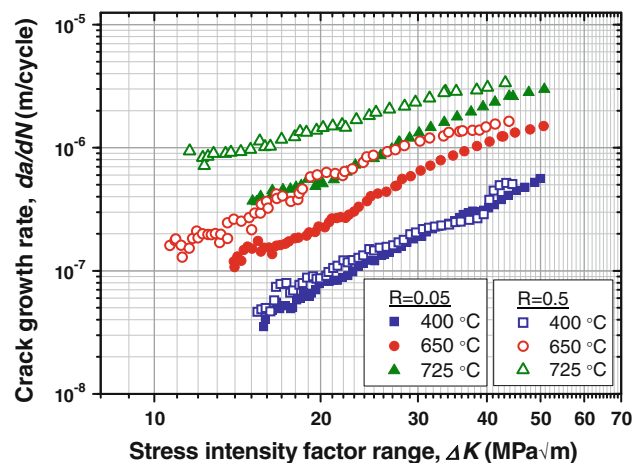
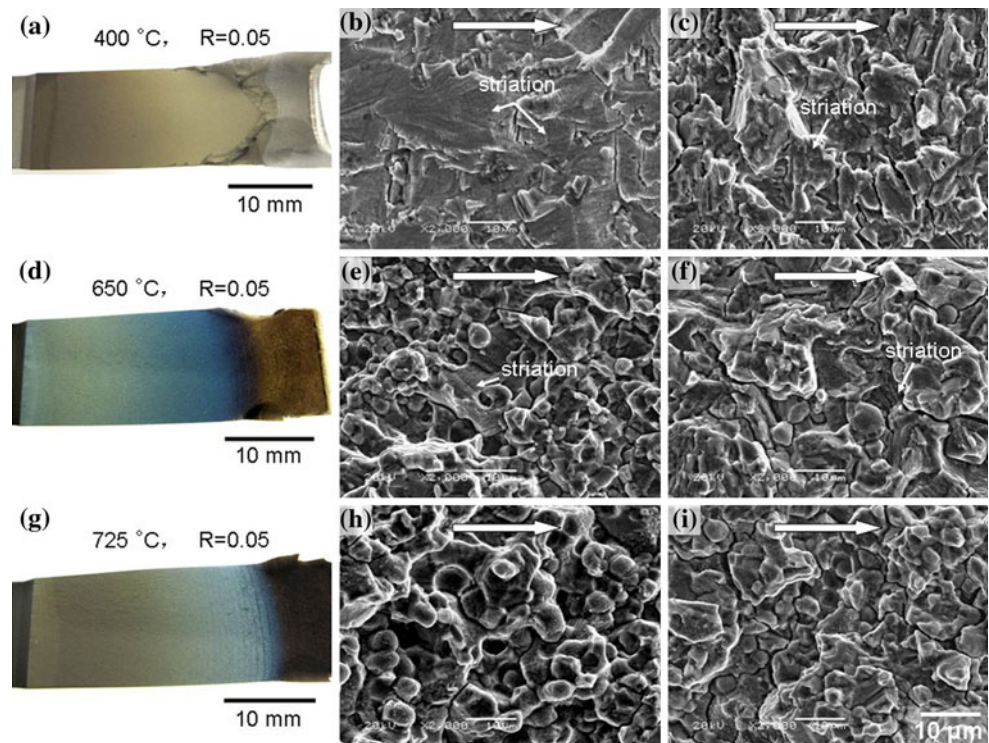


Fig. 4 FCG rate, da/dN , for TMW-4M3 tested with different test temperatures and R values. Note the significant effect of R on FCG rate above $650 \text{ }^\circ\text{C}$

Fig. 5 Fracture surfaces of TMW-4M3 tested under a load ratio of 0.05 at **a** 400 °C, photograph; **b** 400 °C, $\Delta K = 20 \text{ MPa}\sqrt{\text{m}}$; **c** 400 °C, $\Delta K = 40 \text{ MPa}\sqrt{\text{m}}$; **d** 650 °C, photograph; **e** 650 °C, $\Delta K = 20 \text{ MPa}\sqrt{\text{m}}$; **f** 650 °C, $\Delta K = 40 \text{ MPa}\sqrt{\text{m}}$; **g** 725 °C, photograph; **h** 725 °C, $\Delta K = 20 \text{ MPa}\sqrt{\text{m}}$; **i** 725 °C, $\Delta K = 40 \text{ MPa}\sqrt{\text{m}}$. The arrow indicates the crack propagation direction



was also observed (Fig. 5b). Also, the spacing between striations increased as ΔK increased, implying a higher rate of crack growth. The fracture modes observed at higher temperatures were very different from those observed at 400 °C. At 650 °C, a transgranular fracture mode mixed with an intergranular cracking mode was observed. Fine striations were discernible on the fracture surfaces (Fig. 5e, f). Some scattered voids observed at $\Delta K = 20 \text{ MPa}\sqrt{\text{m}}$ regime is thought to be due to fracture/pullout of primary γ' and/or carbides during the test. However, such feature was not observed at $\Delta K = 40 \text{ MPa}\sqrt{\text{m}}$ regime. As the temperature increased to 725 °C, a mixture of transgranular and intergranular fracture mode with an increased proportion of intergranular fracture was observed (Fig. 5h, i). Finally, it is of interest to note that a higher level of secondary cracking occurs at higher ΔK . This is attributed to the need for rapid energy dissipation by the advancing crack. Such energy dissipation is possible by fracture along additional planes, as the crack growth rate increases.

In addition, evidence of cavities normally observed in typical creep cases was not found. Oxidation on the fracture surfaces tested at 650 and 725 °C was observed (Fig. 5d, g), which may adversely affect the crack growth rate by its action on the grain boundaries.

Test under load ratio of 0.5

As mentioned before, the FCG rate is sensitive to the load ratio at elevated temperatures. Thus, the fracture surfaces

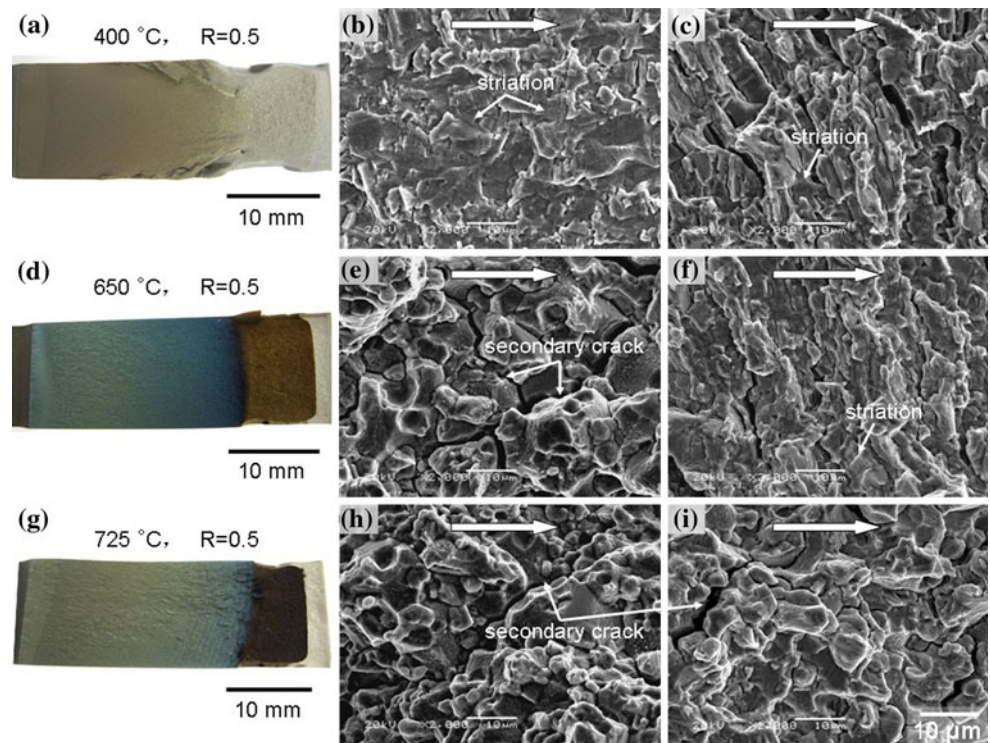
obtained at a higher load ratio of 0.5 were also examined, and the results are given in Fig. 6. Again, a transition in fracture mode from transgranular (400 °C) to mixed transgranular and intergranular (650 °C) and to predominantly intergranular (725 °C) was observed. It needed to be noted that there is almost no difference in fracture surface morphology throughout the Paris regime for 725 °C test (Fig. 6h, i). At higher temperatures, secondary grain boundary cracking was also apparent on the fracture surfaces within the Paris regime (Fig. 6e–i), which indicates that cracking preferentially occurred along grain boundaries at high temperature. Again, no cavities that could be associated with creep damage on the fracture surfaces were observed. At each testing temperature, the major differences in fracture surfaces between lower R (0.05) and higher R (0.5) appear to be the level of secondary cracking and the relative proportion of intergranular fracture, and which increased with increasing the load ratio.

Discussion

Effect of temperature

Under a given load ratio, FCG rate increased with increasing the test temperature (Fig. 4), which is in agreement with these observed in most alloys tested in air [6, 7, 14, 15]. This may be attributed to the following reasons: (1) the creep effect at elevated temperatures;

Fig. 6 Fracture surfaces of TMW-4M3 tested under a load ratio of 0.5 at **a** 400 °C, photograph; **b** 400 °C, $\Delta K = 20 \text{ MPa}\sqrt{\text{m}}$; **c** 400 °C, $\Delta K = 40 \text{ MPa}\sqrt{\text{m}}$; **d** 650 °C, photograph; **e** 650 °C, $\Delta K = 20 \text{ MPa}\sqrt{\text{m}}$; **f** 650 °C, $\Delta K = 40 \text{ MPa}\sqrt{\text{m}}$; **g** 725 °C, photograph; **h** 725 °C, $\Delta K = 20 \text{ MPa}\sqrt{\text{m}}$; **i** 725 °C, $\Delta K = 40 \text{ MPa}\sqrt{\text{m}}$. The arrow indicates the crack propagation direction



(2) the mode of deformation around the crack tip; (3) the oxidation at elevated temperatures; and (4) the changes in mechanical properties in terms of σ_y and E . Considering that creep cavities were not observed on the fracture surfaces, the creep damage effect on crack growth might be negligible for the loading conditions employed as reported in Refs. [14, 16]. Although, the substructure that developed ahead of the fatigue cracks was not examined in this study, an insight [17] into the deformation microstructure of a superalloy at room temperature and 550 °C indicated that almost no difference existed in the substructures in the plastic zone at room temperature and 550 °C. Also, the slopes in the $\log - \log da/dN$ versus ΔK plots remain comparable (Table 3), suggesting a similar fracture mechanism. The mode of deformation may, therefore, not be able to account for the observed difference in FCG rate at different temperatures. A likely explanation is that the oxidation effect at elevated temperatures [13, 15, 18–20]. In their investigation of FCG behavior in U720Li at elevated temperatures, Tucker et al. [6] suggested that oxygen caused grain boundary embrittlement and hence accelerated crack growth. Andrieu et al. [20] have shown that oxygen acted to form oxides that caused irreversibility of slip and thereby increasing the crack growth rate at high temperature. In this study, at 650 and 725 °C, the oxygen may react with active elements in fine grained TMW-4M3 (Ti, Al, and Cr) to form oxide at the crack tip and consequently embrittle the grain boundaries. The intergranular propagation and oxide scale were indeed observed on the

fracture surface (Figs. 5, 6). However, a further study on the FCG test in vacuum at elevated temperatures is required to examine the relative contribution of oxidation and which will be addressed in a subsequent article. It is worthwhile to point out that oxide may also induce crack closure that retards the crack growth, especially for the low values of load ratio, as discussed subsequently.

The increase in FCG rate with temperature may also be associated with the decrease in the strength of the material. A number of researchers [17, 21, 22] have attributed the increase of FCG rate with temperature in superalloys to a decrease in the magnitude of the mechanical properties with increasing temperature. Although, it is difficult to make a quantitative assessment of the contribution arising from the degradation in mechanical properties, such behavior may lead to the change in crack growth rate. The Young's modulus corrected FCG rate data obtained for load ratios of 0.05 and 0.5 at various temperatures is plotted against the $\Delta K/E$, in Fig. 7a, b, respectively. It is apparent that FCG rate acceleration is observed with increasing temperature in the case of $R = 0.05$, which means the change in E alone is not capable of describing this effect. In the case of $R = 0.5$, however, the data nearly collapse onto a single curve, suggesting that the FCG rate is controlled predominantly by the degradation of strength. The exact reason why this law is valid for $R = 0.5$ but not for $R = 0.05$ is unclear at present. The changes in slip distribution (homogeneous vs. inhomogeneous) and fracture path (tortuous vs. flat) under different load ratios may

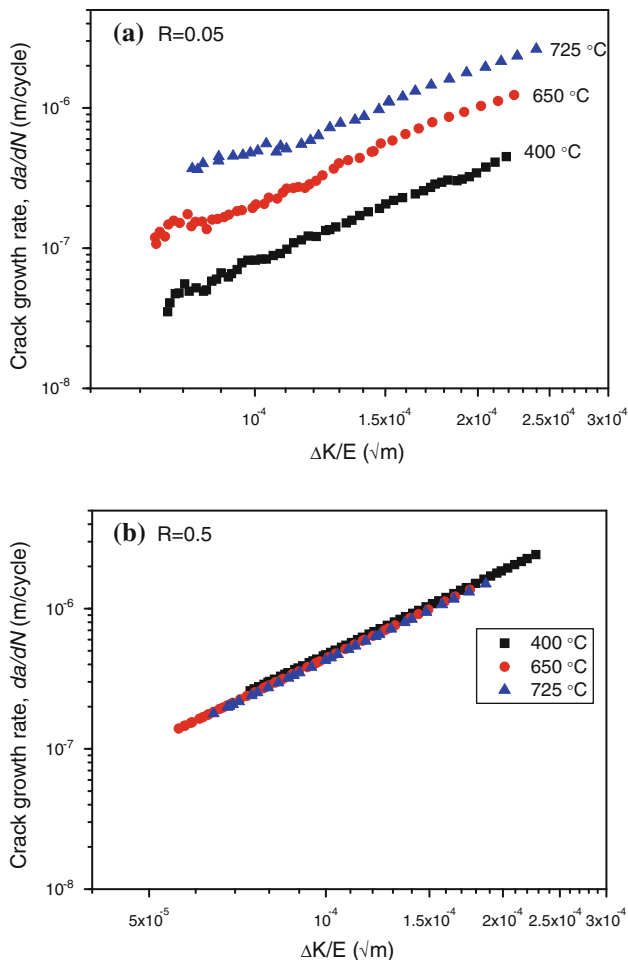


Fig. 7 FCG rate curves of da/dN versus $\Delta K/E$ for different temperatures under R values of **a** 0.05 and **b** 0.5

be account for this behavior [23]. Detailed experimental and modeling studies are required to further understanding of crack growth mechanisms.

Effect of load ratio

At a specific temperature, the FCG rate in TMW-4M3 increased with increasing load ratios. The load ratio effects on FCG rate are commonly explained by the crack closure concept, particularly in the near-threshold regime and at low load ratios [24]. Several mechanisms of crack closure have been discussed in the literatures depending on the material and test conditions. These are mainly in the following four categories; plasticity induced, roughness induced, oxide induced, and transformation induced [25]. In this study, the difference in FCG rate observed at different load ratios may be related to these crack closure mechanisms. However, the relative importance of each of the mechanisms at different temperatures is neglected in this study. Here, the task is made easier, if the variable

R value data can be rationalized into an unified criterion. One method that is commonly used to model variations due to R value is the “Elber” correlation [26]. This is an empirical relationship based on Eq. 3:

$$\Delta K_{eff} = U\Delta K, \tag{3}$$

where ΔK_{eff} is the effective stress intensity factor range, U is the stress intensity ratio. U is given by Eq. 4 assuming U is independent of K_{max} in the Paris regime [27], which is often used for aluminum alloys [28].

$$U = 0.5 + 0.4R. \tag{4}$$

The closure corrected growth rates for each temperature are shown in Fig. 8. Clearly, while the Elber relationship works well at 650 °C for R values of 0.05 and 0.5, at 400 and 725 °C data it is less effective. This suggests that simply assuming U to be independent of temperature and ΔK is inappropriate. A previous study [29] showed that U increased with increasing the load ratio and ΔK , and closure was very insignificant in the case of $R = 0.5$ for Ti-6Al-4V alloy at room temperature. Although, there is a limitation by using the above simple evaluation method, the better fit curves at 650 and 725 °C than 400 °C may reveal that oxide-induced crack closure did occur at higher temperatures, since oxide scale was observed on the fracture surfaces. A technique for the measurement of crack closure is needed to evaluate the effect of crack closure on FCG rate in TMW-4M3.

Aside from the crack closure effect resulting from oxidation, plasticity, and/or fracture roughness, many studies have been contributed to explain the load ratio-dependence of FCG rates for a number of engineering materials. As the load ratio is increased, the magnitude of the mean tensile stress acting on the crack tip increased, which may change the mechanisms of crack-tip deformation. In addition,

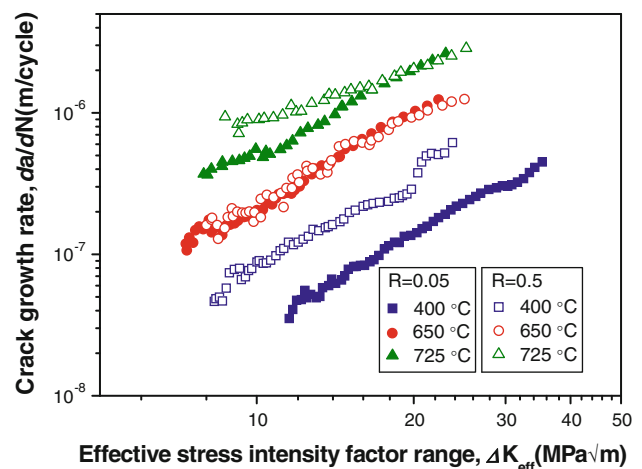


Fig. 8 FCG rate curves of da/dN versus ΔK_{eff} for different temperatures under R values of 0.05 and 0.5

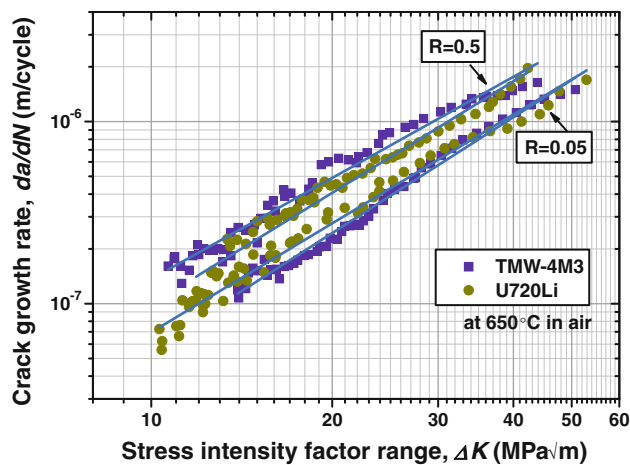


Fig. 9 FCG rate comparison between TMW-4M3 and U720Li tested at 650 °C

under higher R condition the crack remains open for a greater proportion of the loading–unloading cycle, which allows oxygen easy access to the crack tip and subsequently accelerates the crack propagation. Detailed transmission electron microscopy studies would be required to clarify the deformation mode ahead of the crack tip under various conditions.

Another interesting feature for the data under different load ratios is the marked reduction of m value at 725 °C/ $R = 0.5$ (Table 3). A much weaker dependence of crack growth rates on ΔK seems to resemble the distinct feature of corrosion crack growth, where the environment controls the crack propagation rate irrespective of the stress intensity factor level. As mentioned earlier, there was almost no difference in the morphology throughout the fracture surfaces at 725 °C/ $R = 0.5$ (Fig. 6h, i), in contrast to the evident discrepancy under other test conditions. It is, therefore, possible that the rate of crack growth was governed by the oxidation at 725 °C/ $R = 0.5$. Again, the mechanisms of crack-tip deformation are needed to be clarified to verify this postulation.

Comparison of FCG rates between TMW-4M3 and U720Li

It is worth comparing the FCG rates of alloy TMW-4M3 with the results obtained on the commercial superalloy U720Li. The U720Li specimen was fabricated by the same process as for TMW-4M3. This alloy is used for turbine disks and was evaluated at 650 °C with load ratio of 0.05 and 0.5 in FCG tests. Such a comparison is of great interest because both alloys exhibit similar grain structure and volume fraction of γ' and TMW-4M3 is a candidate material to replace U720Li for turbine disk applications. Figure 9 shows the influence of load ratio on FCG rate for

both alloys at 650 °C. As can be seen, the FCG resistance of TMW-4M3 is comparable to that of U720Li. This might be understood in terms of their similar chemical compositions and microstructure.

Conclusions

This investigation was focused on the FCG behavior of TMW-4M3 superalloy under cyclic loading in air environment, and the influences of temperature and load ratio on the FCG rate have been studied. The main results and conclusions could be drawn from this study as follows:

1. The FCG rate increased with increasing the test temperature in TMW-4M3, and which was accompanied by a transition in fracture mode from transgranular (400 °C) to mixed transgranular and intergranular (650 °C), and to predominantly intergranular (725 °C).
2. In the case of $R = 0.05$, the FCG rate increases with increasing the temperature. This behavior is tentatively explained taking into account the oxidation assisted cracking and the degradation of mechanical properties when temperature increases. In the case of $R = 0.5$, however, the degradation of mechanical properties may play a dominant role in controlling the FCG rate.
3. TMW-4M3 superalloy shows a significant load ratio-dependence of FCG rates in Paris regime, especially at higher temperatures (650 and 725 °C). With increasing the load ratio the FCG rates increased markedly.
4. The FCG resistance of TMW-4M3 is comparable to that of the commercial superalloy U720Li at elevated temperatures.

Acknowledgements The financial support from NEDO program sponsored by Japanese government and Mitsubishi Heavy Industry, Japan, are appreciated for this research. The authors would like to thank Dr. J. Fujioka and M. Fukuda for their helpful discussion and the Kobe Materials Testing Laboratory, Japan, for its technical support to this study.

References

1. Reed RC (2006) The superalloys: fundamentals and applications. Cambridge University Press, Cambridge
2. Gu YF, Fukuda T, Cui CY, Harada H, Mitsunashi A, Yokokawa T, Fujioka J, Koizumi Y, Kobayashi T (2009) Metall Mater Trans A 40:3047
3. Cui CY, Gu YF, Harada H, Ping DH, Sato A (2006) Metall Mater Trans A 37:3183
4. Gu YF, Cui CY, Ping DH, Harada H, Fukuda T, Fujioka J (2009) Mater Sci Eng A 510–511:250
5. Gu YF, Harada H, Cui CY, Ping DH, Sato A, Fujioka J (2006) Scr Mater 55:815
6. Tucker AM, Henderson MB, Wilkinson AJ, Hide NJ, Reed PAS (2002) Mater Sci Technol 18:349

7. Evans WJ, Jones JP, Williams S (2005) *Int J Fatigue* 27:1473
8. Arslan G, Doruk M (1998) *J Mater Sci* 33:2653. doi:[10.1023/A:1004369622557](https://doi.org/10.1023/A:1004369622557)
9. Cui CY, Gu YF, Harada H, Sato A (2005) *Metall Mater Trans A* 36:2921
10. Annual Book of ASTM Standards, E21 (2005) ASTM. West Conshohocken, PA
11. Annual Book of ASTM Standards, E647 (2005) ASTM. West Conshohocken, PA
12. Annual Book of ASTM Standards, E399 (1997) ASTM. West Conshohocken, PA
13. Mercer C, Shademan S, Soboyejo WO (2003) *J Mater Sci* 38:291. doi:[10.1023/A:1021161532639](https://doi.org/10.1023/A:1021161532639)
14. Dalby S, Tong J (2005) *J Mater Sci* 40:1217. doi:[10.1007/s10853-005-6940-2](https://doi.org/10.1007/s10853-005-6940-2)
15. Tong J, Dalby S, Byrne J (2005) *J Mater Sci* 40:1237. doi:[10.1007/s10853-005-6942-0](https://doi.org/10.1007/s10853-005-6942-0)
16. Liu HW, McGowan J (1981) *Scr Metall* 16:507
17. Clavel M, Pineau A (1978) *Metall Trans A* 9:471
18. Molins R, Hochstetter G, Chassaing JC, Andrieu E (1997) *Acta Mater* 45:663
19. Tong J, Dalby S, Byrne J, Henderson MB, Hardy MC (2001) *Int J Fatigue* 23:897
20. Andrieu E, Molins R, Ghonem H, Pineau A (1992) *Mater Sci Eng A* 154:21
21. Ghonem H, Nicholas T, Pineau A (1993) *Fatigue Fract Eng Mater Struct* 16:565
22. Osinkolu GA, Onofrio G, Marchionni M (2003) *Mater Sci Eng A* 356:425
23. King JE (1987) *Mater Sci Technol* 3:750
24. Ishihara S, Goshima T, Yoshimoto Y, Sabu T, Mcevely AJ (2000) *J Mater Sci* 35:5661. doi:[10.1023/A:1004846205548](https://doi.org/10.1023/A:1004846205548)
25. Suresh S (1991) *Fatigue of materials*. Cambridge University Press, Cambridge
26. Elber V (1971) In: *Damage tolerance in aircraft structures*. ASTM STP 486, Philadelphia
27. McClung RC (1991) *Metall Trans A* 22:1559
28. Shih TT, Wei RP (1974) *Eng Fract Mech* 6:19
29. Dubey S, Soboyejo ABO, Soboyejo AB (1997) *Acta Mater* 45:2777